International Journal of
Molecular Sciences

MDPI

Article

Airborne Exposure of the Cornea to PM_{10} Induces Oxidative Stress and Disrupts Nrf2 Mediated Anti-Oxidant Defenses

Mallika Somayajulu [1], Sharon A. McClellan [1], Robert Wright [1], Ahalya Pitchaikannu [1], Bridget Croniger [1], Kezhong Zhang [2] and Linda D. Hazlett [1,*]

[1] Department of Ophthalmology, Visual and Anatomical Sciences, School of Medicine, Wayne State University, 540 E. Canfield, Detroit, MI 48201, USA
[2] Center for Molecular Medicine and Genetics, Wayne State University School of Medicine, 540 E. Canfield, Detroit, MI 48201, USA
* Correspondence: lhazlett@med.wayne.edu; Tel.: +(313)-577-1079; Fax: +(313)-577-3125

Abstract: The purpose of this study is to test the effects of whole-body animal exposure to airborne particulate matter (PM) with an aerodynamic diameter of <10 μm (PM_{10}) in the mouse cornea and in vitro. C57BL/6 mice were exposed to control or 500 $\mu g/m^3$ PM_{10} for 2 weeks. In vivo, reduced glutathione (GSH) and malondialdehyde (MDA) were analyzed. RT-PCR and ELISA evaluated levels of nuclear factor erythroid 2-related factor 2 (Nrf2) signaling and inflammatory markers. SKQ1, a novel mitochondrial antioxidant, was applied topically and GSH, MDA and Nrf2 levels were tested. In vitro, cells were treated with $PM_{10} \pm$ SKQ1 and cell viability, MDA, mitochondrial ROS, ATP and Nrf2 protein were tested. In vivo, PM_{10} vs. control exposure significantly reduced GSH, corneal thickness and increased MDA levels. PM_{10}-exposed corneas showed significantly higher mRNA levels for downstream targets, pro-inflammatory molecules and reduced Nrf2 protein. In PM_{10}-exposed corneas, SKQ1 restored GSH and Nrf2 levels and lowered MDA. In vitro, PM_{10} reduced cell viability, Nrf2 protein, and ATP, and increased MDA, and mitochondrial ROS; while SKQ1 reversed these effects. Whole-body PM_{10} exposure triggers oxidative stress, disrupting the Nrf2 pathway. SKQ1 reverses these deleterious effects in vivo and in vitro, suggesting applicability to humans.

Keywords: particulate matter; Nrf2; SKQ1; cornea; mouse

Citation: Somayajulu, M.; McClellan, S.A.; Wright, R.; Pitchaikannu, A.; Croniger, B.; Zhang, K.; Hazlett, L.D. Airborne Exposure of the Cornea to PM_{10} Induces Oxidative Stress and Disrupts Nrf2 Mediated Anti-Oxidant Defenses. *Int. J. Mol. Sci.* **2023**, *24*, 3911. https://doi.org/10.3390/ijms24043911

Academic Editors: Stephen C. Pflugfelder and Cintia S. De Paiva

Received: 10 January 2023
Revised: 3 February 2023
Accepted: 13 February 2023
Published: 15 February 2023

1. Introduction

Air pollution is a major contributor to health problems worldwide [1]. The World Health Organization (WHO) air quality model demonstrates that ambient air pollution annually causes 4.2 million deaths, and 91% of the world's population lives in places where air quality exceeds the limits of WHO guidelines [2]. Epidemiological evidence shows adverse health effects associated with exposure to airborne particulate matter with a mean aerodynamic diameter of <10 μm (PM_{10}) [3]. Long-term exposure is associated with increased risk of cardiovascular [4], cerebrovascular [5], pulmonary diseases [6], arteriosclerosis [7], and cancer [8], while short-term exposure can lead to asthma [9], bronchitis [10], and other respiratory ailments [11]. The effects of PM_{10} have largely focused on the lungs [12–14]. However, very little is known about the effects of PM_{10} on the cornea, which is also readily exposed to this pollutant. Epidemiological and clinical data suggest that air pollution in which PM is a major constituent can cause transient ocular allergies (redness, discharge, foreign body sensation, and itching) [15]. Clinically, dry eye caused by particulates, is a global problem [16]. In this regard, studies from South Korea showed that high PM_{10} exposure correlated with increased outpatient visits for ocular diseases, including emergency room visits for keratitis [17]. A recent study in mice examined the effects of air pollution in Argentina and found that exposure to polluted air compromised corneal immunity and worsened inflammation in acute herpes simplex keratitis [18]. In fact, dry eye [19–22] and conjunctivitis [23,24] are linked (causative or makes the disease

worse), in general, to the effects of air pollution increasing susceptibility to infection. Additionally, a new study in mice examined the effects of particulate matter in China and showed that exposure to particulates contributed to the initiation and advancement of ocular hypertension and glaucoma [25].

Exposure to PM_{10} induces oxidative stress [26] and the generation of free radical species [27]. This oxidative stress has been attributed to PM_{10} components including polycyclic aromatic hydrocarbons [28], ambient ultrafine particles [29] and transition metals such as iron [30]. In fact, metals present in particulate matter can enter mitochondria and perturb mitochondrial membrane potential and induce mitochondrial reactive oxygen species (ROS) and induce apoptosis [31]. Oxidative stress can activate nuclear factor erythroid-2-related factor 2 (Nrf2), a redox-sensitive transcription factor that regulates the expression of downstream anti-oxidant genes and phase-II enzymes that counter ROS and thus protect from adverse biological outcomes [32]. However, repeated and prolonged exposure to polycyclic aromatic hydrocarbons has been shown to inactivate the Nrf2 signaling pathway causing impaired mitochondrial redox homeostasis and leading to mitochondrial dysfunction [33]. In this regard, SKQ1 (10-(6′-plastoquinonyl) decyltriphenylphosphonium) is a mitochondria-specific anti-oxidant that can cross the plasma membrane and accumulate in the inner mitochondrial membrane where it is reduced or recharged in a controlled fashion and surpasses the efficacy of traditional anti-oxidants [34]. The conversion between the oxidized and reduced forms of SKQ1 helps mitigate the damage induced by mitochondrial ROS [35,36]. Studies have shown SKQ1 to be protective against damage from oxidative stress in animal models of ischemia/reperfusion [37], aging [38] and neurodegenerative diseases [39]. Additionally, SKQ1 has been formulated as an eye drop (Visomitin) in Russia and has been shown to prevent anesthesia-induced dry eye syndrome in patients who underwent long-term general anesthesia or ocular surgery [40]. Recently, it has been reported to have undergone a phase 3 clinical trial for the treatment of dry eye disease in the USA [41]. The aim of this study is to understand the effects of PM_{10} in vivo on the normal mouse cornea and in vitro in human corneal epithelial cells with an emphasis on the protective role of SKQ1 as an anti-oxidant and a cytoprotective agent with clinical potential.

2. Results

2.1. PM_{10} Exposure: Tear Secretion and Corneal Sensitivity

The effects of whole-body exposure to PM_{10} vs. control on tear secretion and corneal sensitivity at 0 (pre-exposure) and 2 weeks (post-exposure) are shown in Figure 1A–C. No differences in tear volume of PM_{10} vs. control exposed mice were detected at the 2 weeks time period as observed by the phenol-red thread images (Figure 1A) and tear volume represented as a bar graph in Figure 1B. No significant differences in corneal sensitivity were observed between PM_{10} vs. control exposed groups (Figure 1C) at 2 weeks of exposure.

2.2. Effects of PM_{10} on GSH and MDA Levels and Histopathology

Levels of GSH were significantly lower ($p < 0.05$) after 2 weeks of exposure to PM_{10} vs. control (Figure 2A). Levels of MDA (Figure 2B) were significantly increased ($p < 0.05$) in PM_{10} vs. control exposed corneas at 2 weeks. Because we saw biochemical changes in GSH and MDA levels at 2 weeks of exposure, we next examined paraffin-embedded and hematoxylin and eosin-stained corneas at that time period and the data are shown in Figure 2C. PM_{10} vs. control exposure showed that the epithelium of the cornea was compacted, nuclei in the superficial corneal layers were pynknotic, and infiltrating cells (containing a brownish particulate, Figure 2C inset) were observed in the PM_{10} exposed mice. These cells were easily distinguished due to their distinct cell borders which were visible between corneal epithelial cells which normally are joined by intercellular junctions, including tight junctions. PM_{10} vs. control significantly reduced the thickness of the epithelium (Figure 2D), stroma (Figure 2E) and the entire cornea (Figure 2F, $p < 0.001$ for all).

2.3. Effects of PM_{10} on Innate Immunity

mRNA levels of innate immune markers measured after 2 weeks of exposure to control vs. PM_{10} are shown in Figure 3A–G. mRNA levels were significantly elevated for chemokine (C-X-C) ligand (CXCL)2 (A, $p < 0.001$), Toll-like receptor (TLR)4 (B, $p < 0.001$), TLR2 (C, $p < 0.05$), interleukin (IL)-6 (D, $p < 0.01$), and IL-1β (E, $p < 0.01$) in PM_{10} vs. control exposed animals. No significant differences were observed in the levels of tumor necrosis factor (TNF)-α (F) and receptor for advanced glycation end products (RAGE) (G) in PM_{10} vs. control animals.

2.4. Response to PM_{10}: Nrf2, GSH Maintenance enzymes and Effects of SKQ1 on Oxidative Stress

mRNA levels of GSH maintenance enzymes are shown in Figure 4A–D. Significantly elevated mRNA levels were observed for GSH maintenance enzymes: glutathione peroxidase (GPX) 1 (B, $p < 0.01$), GPX2 (C, $p < 0.01$) and glutathione reductase (GR)1 (D, $p < 0.001$); while Nrf2 (A) levels did not change in PM_{10} vs. control exposure at 2 weeks. Figure 4E–G indicates levels of GSH, MDA and Nrf2 protein after 2 weeks of PM_{10} vs. control exposure and the effects of the mitochondrial anti-oxidant SKQ1. Figure 4E shows a significant decrease ($p < 0.01$) in GSH levels after 2 weeks of PM_{10} vs. control exposure which are significantly reversed ($p < 0.01$) by SKQ1 treatment. MDA levels were significantly increased ($p < 0.01$) after PM_{10} vs. control exposure, and treatment with SKQ1 significantly decreased ($p < 0.001$) MDA levels. Nrf2 protein levels were significantly (<0.01) after PM1- vs. control exposure and SKQ1 restores Nrf2 levels almost to the control level ($p < 0.05$).

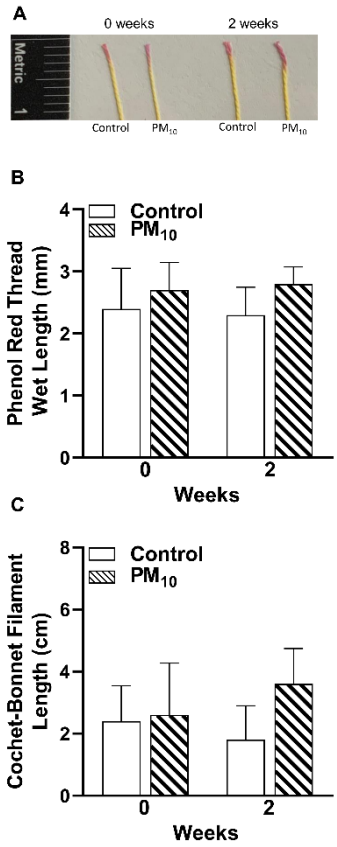

Figure 1. Effects of PM_{10} exposure on tear secretion and corneal sensitivity. (**A**) Phenol red thread images. Red portion of the thread represents tear volume at 0 and 2 weeks after control or PM_{10} exposure. (**B**) The wetted length (red portion) was measured and represented as a bar graph, showed no differences in tear volume. (**C**) Corneal sensitivity was measured using a Cochet-Bonnet Esthesiometer, showed no significant changes between control and PM_{10} groups. Data are expressed as mean + SD. (n = 5/group/time).

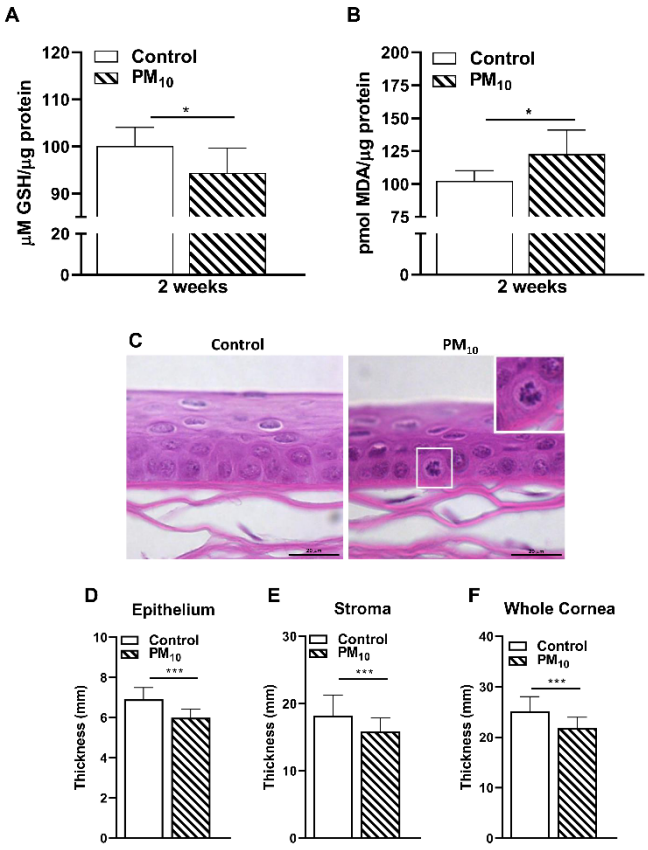

Figure 2. Effects of PM_{10} exposure: oxidative stress and histology. (**A**) Levels of GSH were significantly lower after 2 weeks exposure to PM_{10} vs. control. (**B**) MDA levels (lipid peroxidation end product) were significantly increased in PM_{10} vs. control exposed corneas after 2 weeks. (**C**) Paraffin embedded and hematoxylin and eosin stained corneas after 2 weeks exposure to PM_{10} or control. Inset shows an infiltrating cell containing a brownish particulate. Scale bar = 20 μm. Thickness of the epithelium (**D**), stroma (**E**) and the whole cornea (**F**) were significantly decreased in PM_{10} vs. control exposed corneas. Data are expressed as mean + SD. (* $p < 0.05$, $n = 5$/group (**A**,**B**) *** $p < 0.001$, $n = 3$/group (**D**–**F**)).

2.5. Effects of SKQ1 on Cell Viability, Oxidative Stress, Mitochondrial ROS, ATP and Nrf2 Levels after PM_{10} Exposure in HCET

Phase contrast images of HCET exposed to 100 μg/mL of PM_{10} in the presence or absence of SKQ1 are shown (Figure 5A–C). Figure 5A shows that in the media control group, without PM_{10}, cells are spindle-shaped with prominent nuclei. PM_{10}-exposed cells appear to be thinned with a few rounded cells, and the nuclei are difficult to see (Figure 5B). In the presence of SKQ1, PM_{10}-exposed cells appear similar to the media control group, with spindle-shaped cells and prominent nuclei (Figure 5C). HCET exposed to 100μg/mL PM_{10} in the absence of SKQ1 showed significantly lower ($p < 0.001$) cell viability vs. media control (Figure 5D). Pre-treatment with SKQ1 significantly increased ($p < 0.001$) the viability of cells exposed to 100 μg/mL PM_{10}. Viability was further reduced ($p < 0.001$) when cells were treated with 200 μg/mL PM_{10} vs. media control. However, at 200 μg/mL PM_{10}, SKQ1 treatment was unable to positively affect cell viability. MDA levels were significantly increased ($p < 0.01$) in PM_{10} exposed vs. media control (Figure 5E). SKQ1 significantly reduced ($p < 0.05$) MDA levels in the PM_{10}-exposed cells (Figure 5E). Figure 5F shows that the levels of mitochondrial ROS were significantly increased ($p < 0.001$) by PM_{10} vs. media control. Pre-treatment with SKQ1 significantly reduced ($p < 0.001$) levels of mitochondrial ROS (Figure 5F). PM_{10} vs. media control levels significantly lowered ($p < 0.001$) ATP (Figure 5G). SKQ1 significantly restored ($p < 0.001$) ATP levels in PM_{10}-exposed cells (Figure 5G). The protein levels of Nrf2 measured by Western blot and the

integrated density values (IDV) after normalizing Nrf2 to β-tubulin are represented in Figure 5H. Data indicate a significant reduction ($p < 0.001$) in PM_{10} exposed cells vs. media control. Pre-treating HCET with SKQ1 significantly restored ($p < 0.001$) Nrf2 levels after PM_{10} exposure (Figure 5H).

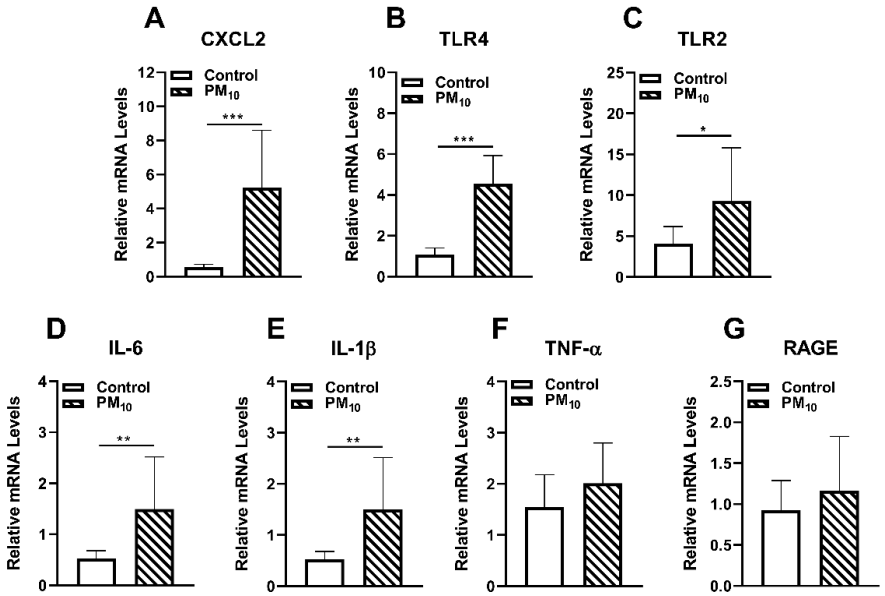

Figure 3. Effects of PM_{10} on innate immunity. RT-PCR showed significantly elevated mRNA levels in PM_{10} vs. control exposed corneas for chemokine CXCL2 (**A**), TLR4 (**B**), TLR2 (**C**), IL-6 (**D**), IL-1β (**E**) only but not TNF-α (**F**) and RAGE (**G**) after 2 weeks exposure. Data are expressed as mean + SD. (* $p < 0.05$, ** $p < 0.01$, *** $p < 0.001$, $n = 5$/group).

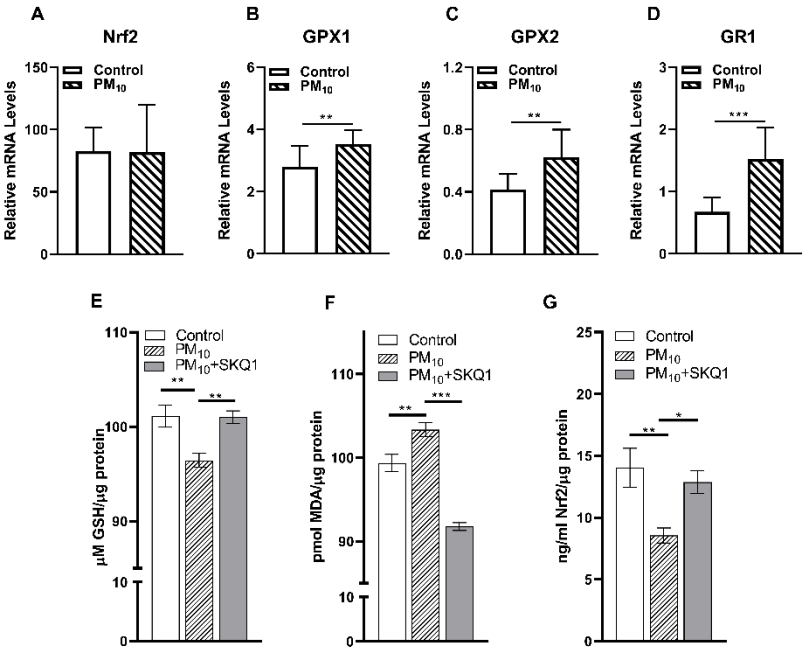

Figure 4. Effects of PM_{10} on Nrf2, GSH maintenance enzymes; protective effects of SKQ1. mRNA levels for GSH maintenance enzymes: GPX1 (**B**), GPX2 (**C**) and GR1 (**D**) are significantly increased in PM_{10} vs. control exposure at 2 weeks; no change for Nrf2 (**A**) levels. Effects of mitochondrial anti-oxidant SKQ1 on the levels of GSH, MDA and Nrf2 proteins after 2 weeks of PM_{10} vs. control exposure (**E**–**G**). SKQ1 protects corneas by significantly increasing GSH (E), reducing MDA (F) and restoring Nrf2 (G) levels. Data are expressed as mean + SD. (* $p < 0.05$, ** $p < 0.01$, *** $p < 0.001$, $n = 5$/group).

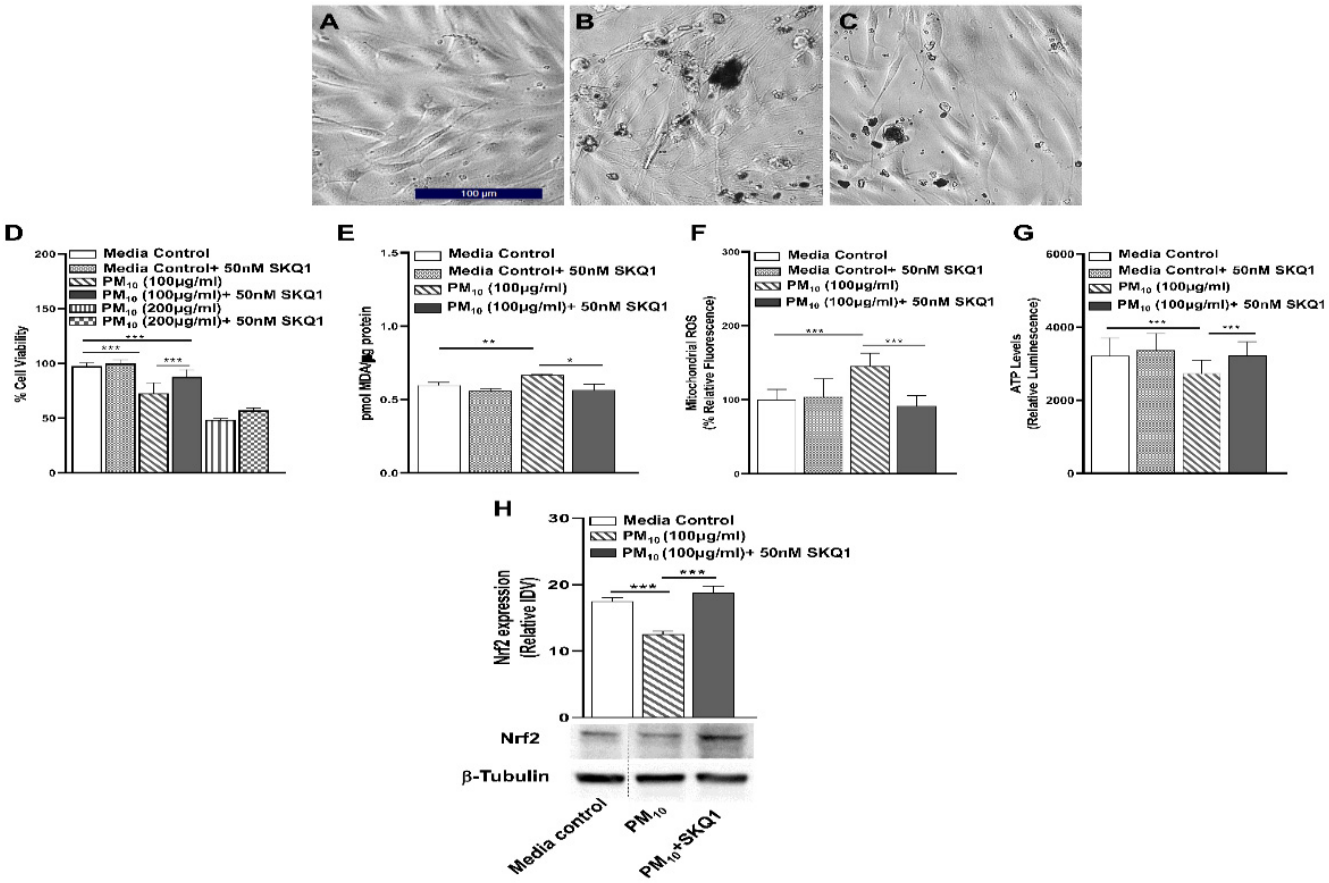

Figure 5. In vitro effects of SKQ1 on transformed HCET: morphology, viability, oxidative stress, Nrf2 protein, mitochondrial ROS and ATP after PM_{10} exposure. (**A**) Phase contrast images of cells in the media control group show elongated cells with prominent nuclei. (**B**) Cells exposed to PM_{10} are thinned and a few rounded cells are seen. (**C**) SKQ1 pre-treated cells appear spindle-shaped with prominent nuclei, similar to media control. Scale bar = 100 µm. (**D**) Exposure to 100 and 200 µg/mL PM_{10} significantly decreased cell viability vs. media control. SKQ1 pretreatment significantly increased cell viability only at 100 µg/mL but not at 200 µg/mL PM_{10}. (**E**) MDA levels were significantly reduced by SKQ1 after exposure to PM_{10}. (**F**) Elevated mitochondrial ROS after PM_{10} exposure was significantly reduced by SKQ1. (**G**) Reduced ATP levels due to PM_{10} exposure were restored by SKQ1. (**H**) Western blot analysis of Nrf2 protein showed that SKQ1 significantly restored Nrf2 levels after PM_{10} exposure. Data are expressed as mean + SD. (* $p < 0.05$, ** $p < 0.01$, *** $p < 0.001$, $n = 3$).

2.6. Effects of SKQ1 on Cell Viability and Nrf2 Levels after PM_{10} Exposure in HCEC

Since we used immortalized corneal epithelial cells (HCET) to study the effects of PM_{10}, we next tested the toxic effects of PM_{10} on primary human corneal epithelial cells (HCEC). A significant reduction ($p < 0.001$) in HCEC cell viability was observed upon exposure to 100 µg/mL PM_{10} vs. media control (Figure 6A). SKQ1 pre-treatment significantly improved ($p < 0.001$) the viability after PM_{10} exposure in HCEC (Figure 6A). Western blot analysis showed that PM_{10} vs. media control significantly reduced ($p < 0.001$) the protein levels of Nrf2 (Figure 6B). SKQ1 pre-treatment significantly increased ($p < 0.01$) Nrf2 levels after PM_{10} exposure vs. PM_{10} without SKQ1 (Figure 6B).

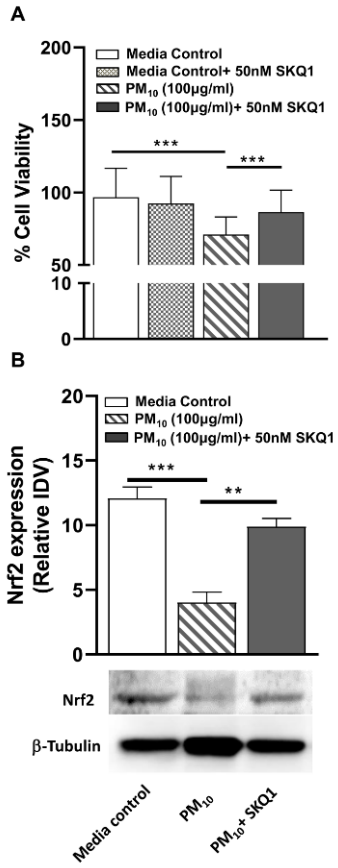

Figure 6. In vitro effects of SKQ1 on cell viability and Nrf2 levels after PM_{10} exposure in primary human corneal epithelial cells (HCEC). (**A**) Loss in cell viability due to PM_{10} exposure was significantly restored by SKQ1 pretreatment. (**B**) Western blot analysis for Nrf2 showed SKQ1 significantly increased Nrf2 levels after PM_{10} exposure. Data are expressed as mean + SD (** $p < 0.01$, *** $p < 0.001$, $n = 3$).

3. Discussion

Exposure of the ocular surface to air pollutants can cause significant irritation and discomfort to the eye [24]. While eye diseases do not affect life expectancy, they nonetheless result in a significant reduction in the quality of life [24]. One such condition is dry eye disease, which is triggered by an array of factors, including tear film instability, and is often associated with elevated tear osmotic pressure and ocular inflammation [42]. Epidemiological studies have implicated the role of air pollution in dry eye disease [43] but the exact mechanism by which PM exerts its toxic effects on the cornea is still not completely understood. Different animal models have been developed to study the effects of PM on the eye using topical eye drops [44,45]; however, the topical application does not reflect actual environmental exposure to particulates. To overcome this limitation, we used a whole-body aerosol exposure system to disperse PM_{10}, a well-characterized product purchased from the National Institute of Standards and Technology (NIST, SRM 2787) [46].

A study using PM_{10} drops at a very high concentration (5 mg/mL, 4X/day) showed reduced tear volume, damaged tear film, impaired ocular surface and reduced goblet cell number in the conjunctiva in male BALB/c mice [47]. However, when we examined the effects of PM_{10} exposure (500 $\mu g/m^3$ in a whole body exposure chamber) on tear secretion, no significant change in tear volume was observed after 2 weeks of exposure. Our results also differ from a recent study in female rats exposed to PM in an exposure chamber (500 $\mu g/m^3$ for 2 weeks) that showed a significant reduction in tear volume after 14 days [48]. These differences could be due to the type of particulates used (we used SRM 2787 vs. samples from China), the time of exposure (3 h/d vs. 5 h/d) and different species

(mice vs. rats). Reduced corneal sensitivity is another characteristic of dry eye disease in patients [49]. However, we did not see any alterations in corneal sensitivity after 2 weeks of PM_{10} exposure. Very little is known about the effects of PM_{10} on corneal sensitivity in animal models. In our study, histological evaluation of PM_{10}-exposed corneas showed pynknotic nuclei and infiltration of inflammatory cells in the epithelium of the cornea. Our data are similar to a previous study that showed increased apoptosis and the infiltration of inflammatory cells in the central cornea of mice that received drops of PM_{10} (5 mg/mL) for 2 weeks [47]. Furthermore, we observed that PM_{10}-exposed corneas exhibited a reduction in the thickness of the epithelium, stroma and the whole cornea. These data are similar to a previous study that examined the effects of the long-term exposure of PM eye drops (5 mg/mL 4x/d) on the cornea, conjunctiva and retina in rats and found a decreased thickness of the epithelium and whole cornea [40]. To understand how PM_{10} exerts its toxicity on the cornea, we then evaluated levels of oxidative stress and inflammation. Our data showed increased pro-inflammatory cytokines and innate immune response markers in the mouse cornea after PM_{10} exposure. Similar effects of PM_{10} on pro-inflammatory cytokine levels have been reported in the eyes of mice that received PM_{10} eye drops for 2 weeks [47]. In addition, we also observed that PM_{10} induced oxidative stress (increased MDA levels) by disrupting the anti-oxidant capacity (decreased GSH levels) in the cornea. In this regard, increased lipid peroxidation and reduced GSH levels have been previously reported in the lungs of rats after PM_{10} instillation [50]. GSH maintenance and synthesis are regulated by the Nrf2 signaling pathway [51]. Nrf2 regulates the rate of GSH synthesis by controlling the activity of the enzymes required for synthesis namely γ-glutamyl cysteine ligase and glutathione synthetase [51] and also controls GSH maintenance by regulating GPX [52], and GR1 [53]. In our study, PM_{10} exposure increased the transcript levels of GPX1, GPX2 and GR1, while Nrf2 levels were unchanged in the mouse cornea after 2 weeks. In contrast, reduced protein levels of Nrf2 were observed which are consistent with data from a mouse model of experimental autoimmune encephalomyelitis (EAE) [54]. Interestingly, low Nrf2 protein levels in EAE were not due to a reduced amount of Nrf2 mRNA, which instead slightly increased in the diseased tissue with time. The discrepancy between mRNA and protein levels for Nrf2 was noted and could be due to alterations in translation and/or other unknown post-translational processes of Nrf2 under pathological conditions such as EAE [54].

Ongoing research is focused on developing eye therapeutics to combat the deleterious effects of air pollution on the eye [55,56]. SKQ1 (Visomitin), a novel mitochondria-targeted anti-oxidant has been used to treat inflammation linked to anesthesia-induced dry eye disease and corneal wounds [40]. In experimental models, SKQ1 administered for 5 days at 50 nmol/kg increased mRNA levels of Nrf2 and antioxidant enzyme genes (SOD1, SOD2, CAT, GPX4) in the cerebral cortex of rat brain under normal and hyperoxic conditions [57]. In our study, we tested the efficacy of SKQ1 as a protective agent against the deleterious effects induced by PM_{10} in the mouse cornea. SKQ1 protected the cornea against PM_{10} toxicity by significantly reducing oxidative stress (reducing lipid peroxidation) and restoring levels of anti-oxidant GSH and Nrf2.

Since data generated in a mouse system often does not translate to human applicability, we further tested the effects of PM_{10} and SKQ1 in vitro on transformed and primary human corneal epithelial cells. PM_{10} reduced cell viability in a concentration-dependent manner in transformed corneal epithelial cells. In this respect, PM has been shown to affect cell viability in vitro in a dose-dependent manner in human corneal epithelial cells [58]. We observed that anti-oxidant SKQ1 significantly reversed PM_{10}-induced loss in cell viability. Our study showed that SKQ1 was protective when cells were treated with 100 μg/mL, but not 200 μg/mL of PM_{10}. Therefore, we selected 100 μg/mL PM_{10} as the optimal dose for all further experiments. We further confirmed our findings in primary human corneal epithelial cells and observed that SKQ1 could reverse the toxic effects of PM_{10} on cell viability. The protective effects of SKQ1 on the ocular surface have been previously established [59]. SKQ1 can enhance cell proliferation and boost corneal wound healing

in corneal limbal epithelial cells at a concentration of 50 nM [59]. Furthermore, the study indicated that at higher concentrations, SKQ1 was cytotoxic [59].

Oxidative stress and inflammation have been implicated as the main mechanisms of PM-mediated toxicity [58]. Components of PM such as poly aromatic hydrocarbons and heavy metals can generate reactive oxygen species (ROS) leading to oxidative stress. Mitochondria are the major generators of ROS, but they are also targets of PM toxicity [60]. In this regard, $PM_{2.5}$ can accumulate in the mitochondria, disrupt mitochondrial structure and function, induce mitochondrial ROS and activate the intrinsic apoptotic pathway [32,61]. When we tested PM_{10} toxicity in transformed human corneal epithelial cells; we observed increased lipid peroxidation (MDA), increased mitochondrial ROS and reduced ATP production after PM_{10} treatment. Impaired mitochondrial function, amplified ROS and increased apoptosis have been previously reported in lung epithelial cells treated with oil fly ash [61] or PM samples collected in Milan [62]. Oxidative stress and inflammation induced by acute or chronic exposure to particulates involve Nrf2 signaling [32,63,64]. At low doses or single acute exposure, PM induces Nrf2 expression [63] but at high doses or multiple chronic exposures, may cause an oxidative burst and thus compromise Nrf2 signaling [32,64]. This can acutely damage mitochondrial redox balance and reduce energy levels [32,65]. We treated both transformed and primary human corneal epithelial cells with a high dose (100µg/mL) of PM_{10} and observed a decrease in Nrf2 protein levels. Our data are similar to a study in human alveolar epithelial cells which showed a significant reduction in Nrf2 levels and impairment of GSH after treating cells with 100–500 µg/mL of PM_{10} [50]. Additionally, SKQ1 protected cells from oxidative stress, and mitochondrial dysfunction and restored Nrf2 levels after PM_{10} exposure. In conclusion, we have shown (diagrammatically in Figure 7) that whole-body exposure to PM_{10} triggers oxidative stress and disrupts the Nrf2 pathway in the cornea. SKQ1 treatment reverses these deleterious effects. In vitro human corneal epithelial cell data parallel the in vivo effects.

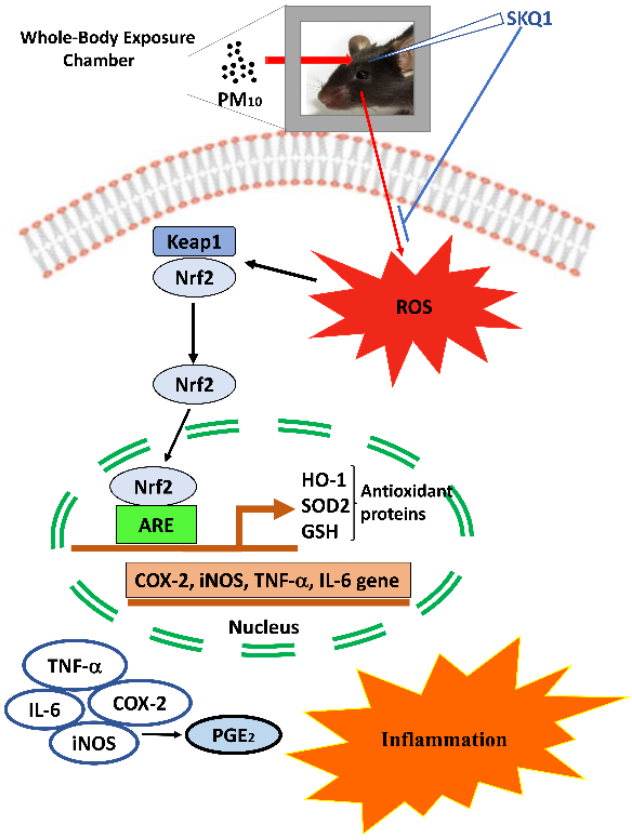

Figure 7. Whole body exposure to PM_{10} is shown diagrammatically.

4. Materials and Methods

4.1. Mice

Eight-week-old C57BL/6 female mice were purchased from the Jackson Laboratory (Bar Harbor, ME, USA) and housed in accordance with the National Institutes of Health guidelines. They were humanely treated and in compliance with both the ARVO Statement for the Use of Animals in Ophthalmic and Vision Research) and the Institutional Animal Care and Use Committee of Wayne State University (IACUC 21-09-4042).

4.2. Whole Body Exposure to PM_{10}

Particulate matter, a major air pollutant is a general term for small atmospheric solid and liquid particles that vary in size (2.5–10 μm), composition and origin [66]. All experiments in this study were performed with PM_{10} purchased from the National Institute of Standards and Technology, (NIST) (Standard Reference Material (SRM) 2787). A whole-body exposure chamber (CH Technologies, Westwood, NJ, USA) was used for all the in vivo experiments performed in this study (Figure 8). Exposures were carried out in a stainless steel, whole-body inhalation chamber; one group was exposed to PM_{10} whereas the other received only humidified compressed air (control). The apparatus is equipped with a Vilnius aerosol generator (VAG), a dry powder dispenser that offers high stability of aerosol output. Mice were exposed to control or an acute, high dose of PM_{10} (500 $\mu g/m^3$) for 2 weeks for 3 h/day/5 days/week and rested on the weekends. For the in vivo study, the dosage was based on mean PM_{10} concentrations measured in the winter, ranging as high as 494 $\mu g/m^3$ in five Chinese cities [67]. For in vitro studies, PM_{10} was used at a concentration of 100 μg/mL as previously published [68,69].

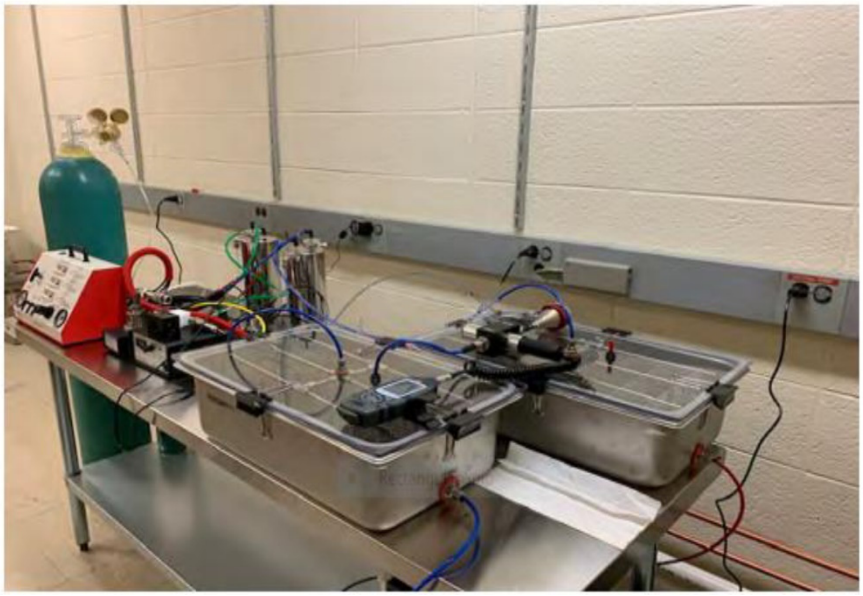

Figure 8. Airborne, whole body particulate matter exposure chamber.

4.3. SKQ1 Treatment

SKQ1 (BOC Sciences, Shirley, NY, USA) was used to treat PM_{10}-exposed mice using a published dose of 7.5 μM [40]. Eyes were treated topically with 5 μL SKQ1 or PBS (control), three times a day before the first chamber exposure and then once each day before exposure for 2 weeks. For in vitro studies, SKQ1 was used at a concentration of 50 nM as previously described [59].

4.4. Endotoxin and Beta-D-Glucan

We are using Standard Reference Material (SRM) 2787 National Institute of Standards and Technology, (NIST) which is one of the most characterized particulate materials for a wide range of organic and inorganic constituents [46].

The mass fractions of the constituents represent those in a contemporary urban environment and complement the mass fractions found in existing SRM. To determine levels of endotoxin, we also tested SRM 2787 using the Pyrochrome Kit for detection and quantification of Gram-negative bacterial endotoxin (Associates of Cape Cod Inc. Falmouth, MA, USA) and endotoxin (*E. coli* O113:H10) to create a standard curve (ACCI). PM_{10} was tested at concentrations of 5 μg/mL, 1 μg/mL, 0.5 μg/mL (equivalent to 500 μg/m^3, used for whole-body exposure), 0.25 μg/mL, and 0.125 μg/mL. All concentrations tested were below the limit of detection (0.005 EU/mL). We also tested for fungal contaminant (1,3)-Beta-D-Glucan using the Glucatell (1,3)-Beta-D-Glucan Kit (Associates of Cape Cod Inc.). PM_{10} was tested at the same concentrations used for testing endotoxin. All concentrations were below the limit of detection (0.625 pg/mL β-glucan standard, not shown). These data assure PM_{10} from NIST is not contaminated by either bacterial or fungal components which would complicate data analysis.

4.5. Tear Secretion

Tear levels were measured in the right eye of the control and PM_{10} exposed mice (n = 5/group/treatment) using Zone-Quick phenol red treated threads (Tianjin Jingming New Technological Development Co., Ltd., Tianjin, China) as described before [70]. Measurements were made before chamber exposure (week 0) to acquire a baseline reading and then at 2 weeks of exposure. Briefly, mice were lightly anesthetized and held while tear levels were measured by placing the tip of a phenol red impregnated cotton thread with a blunt tip on the bulbar conjunctiva (lateral canthus for 30 s). Appropriate care was taken to avoid touch stimulation of eyelashes and whiskers. The wetted length (in millimeters), indicated by a color change from yellow to red, was photographed and measured. Data are shown as mean wetted length + SD.

4.6. Corneal Sensation

Corneal sensitivity was measured for control and PM_{10} exposed mice (n = 5/group/treatment) using a Cochet–Bonnet esthesiometer (Luneau SAS #10129; Prunay-le-Gillon, France) as described before [70]. Measurements were made before chamber exposure (week 0) to acquire a baseline reading and at 2 weeks after exposure. Measurements were made from a filament length of 60 mm and gradually decreased in 5 mm steps to a length of 5 mm. For each filament length, five repeat measurements were conducted. If three blinks were evoked in response to five consecutive touches, a positive response was recorded. The longest filament length which caused a positive response was recorded as the corneal sensitivity threshold. Data are shown as mean filament length + SD.

4.7. Reduced Glutathione (GSH) Assay

Total GSH levels were analyzed by a glutathione assay kit (Cayman Chemical, Ann Arbor, MI, USA) per the manufacturer's protocol and as previously described [71]. Briefly, individual mouse corneas (n = 5/group/treatment) from control vs. PM_{10} exposed groups ± SKQ1 were harvested in 500 μL of ice-cold 50 mM MES (2-(N-morpholino) ethanesulphonic acid) containing 1 mM EDTA, homogenized and centrifuged at 10,000× g at 4 °C for 10 min and the supernatant was collected. Total GSH levels were determined using Ellman's reagent (DTNB, 5,5′-dithio-bis-2-nitrobenzoic acid), which reacts with the sulfhydryl group of GSH resulting in a yellow-colored 5-thio-2-nitrobenzoic acid (TNB) product. Measurement of the absorbance of TNB at 405 nm provides an estimate of GSH in the sample. GSH levels were calculated using a standard curve and then normalized to the total protein in each sample. A Bradford assay was used to determine protein concentration in each sample. Protein levels were calculated using a standard curve with bovine

serum albumin and Bio Rad protein assay reagent (Bio Rad, Hercules, CA, USA) per the manufacturer's protocol. Final GSH levels were expressed as mean + SD.

4.8. ELISA

ELISA kits were used to measure protein levels of Nrf2 (Novus Biologicals, Centennial, CO, USA) and lipid peroxidation end product MDA (Cell Biolabs, San Diego, CA, USA). Briefly, individual mouse corneas (n = 5/group/treatment) from the control vs. PM_{10} exposed groups ± SKQ1 were harvested in 500 µL of PBS containing 0.1% Tween 20 and protease inhibitors. All assays were run per the manufacturer's protocol and data were normalized to total protein (described above) and expressed as mean + SD.

4.9. H&E Staining of Exposed Corneas

Whole eyes (n = 3) were harvested from mice after 2 weeks of exposure to control or 500 µg/m^3 PM_{10}. Eyes were fixed in alcoholic z-fix and sent to Excalibur Pathology, Inc (Norman, OK) where they were embedded in paraffin, sectioned and stained with H&E. Photographs of representative areas of the epithelium were taken using a Leica DM4000B light microscope at 20X. The thickness of the whole cornea, epithelium and stroma were analyzed from three mice in each group (72 measurements/group/treatment). Data are represented as thickness (in mm) and expressed as mean + SD.

4.10. RT-PCR

Total RNA was isolated from control and PM_{10}-exposed mouse corneas (n = 5/group/treatment) (RNA STAT-60; Tel-Test, Friendswood, TX, USA) per the manufacturer's instructions as reported before [72]. Briefly, 1 µg of each RNA sample was reverse transcribed using Moloney-murine leukemia virus (M-MLV) reverse transcriptase (Invitrogen, Carlsbad, CA, USA) to produce a cDNA template and diluted 1:20 using DEPC-treated water. A 2 µL aliquot of diluted cDNA was used for the RT-PCR reaction. SYBR green/fluorescein PCR master mix (Bio-Rad Laboratories, Richmond, CA, USA) and primer concentrations of 10 µM were used in a total 10 µL volume. After a pre-programmed hot start cycle (3 min at 95 °C), PCR amplification was repeated for 45 cycles with parameters: 15 s at 95 °C and 60 s at 60 °C. Levels of chemokine CXCL2, TLR4, TLR2, IL-6, IL-1β, TNF-α, RAGE, Nrf2, GPX1, GPX2, and GR1 were tested by real-time RT-PCR (CFX Connect real-time PCR detection system; Bio-Rad Laboratories). The fold differences in gene expression were calculated relative to housekeeping gene β-actin mRNA and expressed as the relative mRNA concentration + SD. Primer pair sequences used are shown in Table 1.

4.11. Tissue Culture

HCET cells (HCE-2 [50.B1], ATCC, Gaithersburg, MA, USA) were cultured in Keratinocyte-serum free medium (Gibco, Grand Island, NY, USA) with 5 ng/mL human recombinant EGF, 0.05 mg/mL bovine pituitary extract, 0.005 mg/mL insulin, and 500 ng/mL hydrocortisone as reported before [73]. HCEC (primary corneal epithelial cells, ATCC) were cultured in Keratinocyte-serum free medium (Gibco) with 5 ng/mL human recombinant EGF and 0.05 mg/mL bovine pituitary extract as per the manufacturer's protocol. To evaluate the effects of SKQ1, a subset of cells was incubated with 50 nM SKQ1 as previously described [59], 1 h prior to PM_{10} exposure. Phase contrast microscopy was used to photograph cell preparations using a Leica EL 6000 microscope (Deerfield, IL, USA).

4.12. Cell Viability Assay

An MTT 3-(4, 5-dimethylthiazol-2-yl)-2,5-diphenyltetrazolium bromide (ThermoFisher Scientific, Grand Island, NY, USA) assay was used to test the effects of PM_{10} on HCET viability in the presence and absence of SKQ1, per the manufacturer's protocol and as reported before [73]. Briefly, 15,000 HCET cells were seeded in a 96-well plate, treated with increasing concentrations of PM_{10} (0, 100 and 200 µg/mL) ± 50 nM SKQ1 and incubated for 24 h. At the end of the treatments, 5 mg/mL MTT reagent was added to each well

and incubated at 37 °C for 4 h and the media was removed. Dimethyl sulfoxide (DMSO) was added (50 µL/well) and optical density was read at 540 nm using a SpectraMax M5 microplate reader (Molecular Devices, Sunnyvale, CA, USA). The cell viability was tested similarly for HCEC with 0 and 100 µg/mL PM_{10} ± 50 nM SKQ1 after 24 h incubation. Data are shown as % cell viability + SD.

Table 1. Nucleotide sequence of the specific primers used for PCR amplification (Mouse).

Gene	Nucleotide Sequence	Primer	GenBank
B-actin	5′-GAT TAC TGC TCT GGC TCC TAG C-3′	F	NM_007393.3
	5′-GAC TCA TCG TAC TCC TGC TTG C-3′	R	
Tlr2	5′-CTC CTG AAG CTG TTG CGT TAC-3′	F	NM_011905.3
	5′-TAC TTT ACC CAG CTC GCT CAC TAC-3′	R	
Tlr4	5′-CCT GAC ACC AGG AAG CTT GAA-3′	F	NM_021297.2
	5′-TCT GAT CCA TGC ATT GGT AGG T-3′	R	
Il-1β	5′-TGT CCT CAT CCT GGA AGG TCC ACG-3′	F	NM_008361.3
	5′-TGT CCT CAT CCT GGA AGG TCC ACG-3′	R	
Cxcl2	5′-TGT CAA TGC CTG AAG ACC CTG CC-3′	F	NM_009140.2
(*Mip2*)	5′-AAC TTT TTG ACC GCC CTT GAG AGT GG-3′	R	
Gpx1	5′CTC ACC CGC TCT TTA CCTTCC T-3′	F	NM_008160.6
	5′-ACA CCG GAG ACC AAA TGA TGT ACT-3′	R	
Gpx2	5′-GTG GCG TCA CTC TGA GGA ACA-3′	F	NM_030667
	5′-CAG TTC TCC TGA TGT CCG AAC TG-3′	R	
Gr1	5′-CCA CGG CTA TGC AAC ATT CG-3′	F	NM_010344.4
	5′-GAT CTG GCT CTC GTG AGG AA-3′	R	
Il-6	5′-CAC AAG TCC GGA GAG GAG AC-3′	F	NM_031168.1
	5′-CAG AAT TGC CAT TGC ACA AC-3′	R	
Nrf2	5′-TGC CCC TCA TCA GGC CCA GT-3′	F	NM_010902.5
	5′-GCT CGG CTG GGA CTC GTG TT-3′	R	
Rage	5′-AGG CGT GAG GAG AGG AAG GCC-3′	F	NM_007425.2
	5′-TTA CGG TCC CCC GGC ACC AT-3′	R	
Tnf-a	5′-ACC CTC ACA CTC AGA TCA TCT T-3′	F	NM_013693.2
	5′-GGT TGT CTT TGA GAT CCA TGC-3′	R	

F, forward, R, reverse.

4.13. Mitochondrial ROS Assay

Mitochondrial ROS was analyzed by fluorescence with MitoSOX assay (ThermoFisher Scientific) according to the manufacturer's protocol and as previously described [63]. Briefly, 15,000 HCET cells were plated onto 96 well plates, and treated with 100 µg/mL PM_{10} ± 50 nM SKQ1 for 6 h. Cells were washed with PBS and incubated with 10 µM MitoSOX at 37 °C for 10 min. Cells were then washed twice with PBS and fluorescence was measured at 510 nm (excitation) and 590 nm (emission) using SpectraMax M5 spectrophotometer (Molecular Devices). The level of ROS is proportional to fluorescence intensity. Data were normalized to control and are represented as % relative fluorescence + SD.

4.14. Mitochondrial ToxGlo Assay

To determine whether PM_{10} caused a reduction in ATP levels, a mitochondrial ToxGlo assay (Promega, Madison, WI, USA) was performed per the manufacturer's protocol and as previously described [74]. Briefly, 15,000 HCET were plated onto 96 well plates, incubated overnight and media removed. Cells were then incubated galactose supplemented RPMI 1640 media and treated with 100 µg/mL PM_{10} ± 50 nM SKQ1 for 3 h. ATP detection reagent was added to each well, mixed and incubated for 5 min and luminescence was measured. The levels of ATP are represented as relative luminescence. Data are shown as mean + SD.

4.15. Western Blot

HCET or HCEC were treated with 100 µg/mL PM_{10} ± SKQ1 for 24 h, washed with ice-cold 0.1 M PBS (pH 7.4), lysed in RIPA buffer with protease and phosphatase inhibitors

(SantaCruz Biotech, Dallas, TX, USA), incubated on ice for 20 min, centrifuged at 12,000× *g* at 4 °C for 10 min and the supernatant was collected. Total protein was determined from the supernatants using a BCA protein kit (ThermoFisher Scientific). Briefly, samples (75 µg) were run on SDS-PAGE in Tris-glycine-SDS buffer and electro-blotted onto nitrocellulose membranes (BioRad). After blocking for 1 h in 5% MTBST (Tris Buffer Saline containing 0.05% Tween 20 (TBST) and 5% nonfat milk), membranes were probed with primary antibodies: rabbit anti-mouse Nrf2 (1:500; Cell Signaling Technology, Danvers, MA, USA) in 2% MTBST overnight at 4 °C. After three washes with TBST, membranes were incubated with HRP-conjugated anti-rabbit secondary antibody (1:2000; Cell Signaling Technology) and diluted in 5% MTBST at room temperature for 2 h. Bands were developed with Supersignal West Femto Chemiluminescent Substrate (ThermoFisher Scientific), visualized using an iBright™ CL1500 Imaging System (ThermoFisher Scientific), and normalized to β-Tubulin (1:1000; Abcam, Waltham, MA, USA) and the intensity was quantified using ImageJ software. Data are shown as mean integrated density values (IDV) + SD.

4.16. Statistical Analysis

For in vivo data analysis, a one-way ANOVA followed by Bonferroni's multiple comparison test (GraphPad Prism) was used to test the significance of tear production, corneal sensitivity, GSH, and ELISA (Nrf2, MDA). A Student's *t*-test (GraphPad Prism) was used to determine the significance of the thickness of the whole cornea, epithelium, stroma, RT-PCR, GSH assay and ELISA (MDA) in vivo. For analyzing in vitro data, a one-way ANOVA followed by Bonferroni's multiple comparison test (GraphPad Prism) was used to test the significance for MTT, ROS, ATP assay, ELISA (MDA) and Western blot. Data were considered significant at $p < 0.05$. All experiments were repeated at least once to ensure reproducibility and data are shown as mean + SD.

Author Contributions: Conceptualization, L.D.H. and K.Z.; methodology, M.S. and L.D.H.; formal analysis, M.S., R.W. and S.A.M.; investigation, M.S., S.A.M., R.W., A.P. and B.C.; resources, L.D.H. and K.Z.; data curation, M.S.; writing—original draft preparation, M.S. and L.D.H.; writing—review and editing, M.S., S.A.M. and L.D.H.; visualization, M.S. and S.A.M.; supervision, L.D.H.; project administration, L.D.H.; funding acquisition, L.D.H. and K.Z. All authors have read and agreed to the published version of the manuscript.

Funding: This work as supported by NIH grants R01EY016058 and P30EY004068 from the National Eye Institute: National Institutes of Health (LDH), NIH grant DK126908 (KZ), and a Research to Prevent Blindness (RPB) unrestricted grant to the Department of Ophthalmology, Visual and Anatomical Sciences and Kresge Eye Institute.

Institutional Review Board Statement: Mice were humanely treated and in compliance with both the ARVO Statement for the Use of Animals in Ophthalmic and Vision Research) and the Institutional Animal Care and Use Committee of Wayne State University (IACUC 21-09-4042).

Informed Consent Statement: Not applicable.

Data Availability Statement: Not applicable.

Conflicts of Interest: The authors declare no conflict of interest.

References

1. Kelly, F.J. Oxidative stress: Its role in air pollution and adverse health effects. *Occup. Environ. Med.* **2003**, *60*, 612–616. [CrossRef]
2. World Health Organization. Air Pollution. Available online: https://www.who.int/news-room/factsheets/detail/ambient-(outdoor)-air-quality-and-health (accessed on 2 March 2022).
3. Orellano, P.; Reynoso, J.; Quaranta, N.; Bardach, A.; Ciapponi, A. Short-term exposure to particulate matter (PM10 and PM2.5), nitrogen dioxide (NO_2), and ozone (O_3) and all-cause and cause-specific mortality: Systematic review and meta-analysis. *Environ. Int.* **2020**, *142*, 105876. [CrossRef]
4. Stockfelt, L.; Andersson, E.M.; Molnár, P.; Gidhagen, L.; Segersson, D.; Rosengren, A.; Barregard, L.; Sallsten, G. Long-term effects of total and source-specific particulate air pollution on incident cardiovascular disease in Gothenburg, Sweden. *Environ. Res.* **2017**, *158*, 61–71. [CrossRef]

5. Hahad, O.; Lelieveld, J.; Birklein, F.; Lieb, K.; Daiber, A.; Münzel, T. Ambient Air Pollution Increases the Risk of Cerebrovascular and Neuropsychiatric Disorders through Induction of Inflammation and Oxidative Stress. *Int. J. Mol. Sci.* **2020**, *21*, 4306. [CrossRef]
6. Choi, S.B.; Yun, S.; Kim, S.J.; Park, Y.B.; Oh, K. Effects of exposure to ambient air pollution on pulmonary function impairment in Korea: The 2007-2017 Korea National Health and Nutritional Examination Survey. *Epidemiol. Health* **2021**, *43*, e2021082. [CrossRef]
7. Liang, S.; Zhang, J.; Ning, R.; Du, Z.; Liu, J.; Batibawa, J.W.; Duan, J.; Sun, Z. The critical role of endothelial function in fine particulate matter-induced atherosclerosis. *Part. Fibre Toxicol.* **2020**, *17*, 61. [CrossRef]
8. Tseng, C.H.; Tsuang, B.J.; Chiang, C.J.; Ku, K.C.; Tseng, J.S.; Yang, T.Y.; Hsu, K.H.; Chen, K.C.; Yu, S.L.; Lee, W.C.; et al. The Relationship Between Air Pollution and Lung Cancer in Nonsmokers in Taiwan. *J. Thorac. Oncol.* **2019**, *14*, 784–792. [CrossRef]
9. Han, C.H.; Pak, H.; Chung, J.H. Short-term effects of exposure to particulate matter and air pollution on hospital admissions for asthma and chronic obstructive pulmonary disease in Gyeonggi-do, South Korea, 2007–2018. *J. Environ. Health Sci. Eng.* **2021**, *19*, 1535–1541. [CrossRef]
10. Hooper, L.G.; Young, M.T.; Keller, J.P.; Szpiro, A.A.; O'Brien, K.M.; Sandler, D.P.; Vedal, S.; Kaufman, J.D.; London, S.J. Ambient Air Pollution and Chronic Bronchitis in a Cohort of U.S. Women. *Environ. Health Perspect.* **2018**, *126*, 027005. [CrossRef]
11. Zhu, F.; Ding, R.; Lei, R.; Cheng, H.; Liu, J.; Shen, C.; Zhang, C.; Xu, Y.; Xiao, C.; Li, X.; et al. The short-term effects of air pollution on respiratory diseases and lung cancer mortality in Hefei: A time-series analysis. *Respir. Med.* **2019**, *146*, 57–65. [CrossRef]
12. Consonni, D.; Carugno, M.; De Matteis, S.; Nordio, F.; Randi, G.; Bazzano, M.; Caporaso, N.E.; Tucker, M.A.; Bertazzi, P.A.; Pesatori, A.C.; et al. Outdoor particulate matter (PM10) exposure and lung cancer risk in the EAGLE study. *PLoS ONE* **2018**, *13*, e0203539. [CrossRef]
13. Grzywa-Celińska, A.; Krusiński, A.; Milanowski, J. 'Smoging kills'—Effects of air pollution on human respiratory system. *Ann. Agric. Environ. Med.* **2020**, *27*, 1–5. [CrossRef]
14. Han, H.; Oh, E.Y.; Lee, J.H.; Park, J.W.; Park, H.J. Effects of Particulate Matter 10 Inhalation on Lung Tissue RNA expression in a Murine Model. *Tuberc. Respir. Dis.* **2021**, *84*, 55–66. [CrossRef]
15. Schiavi, C.; Giannaccare, G. Eye and Pollution. In *Clinical Handbook of Air Pollution-Related Diseases*, 1st ed.; Capello, F., Gaddi, A., Eds.; Springer: New York, NY, USA, 2018; pp. 341–351.
16. Narayanan, S.; Redfern, R.L.; Miller, W.L.; Nichols, K.K.; McDermott, A.M. Dry eye disease and microbial keratitis: Is there a connection? *Ocul. Surf.* **2013**, *11*, 75–92. [CrossRef]
17. Lee, J.Y.; Kim, J.W.; Kim, E.J.; Lee, M.Y.; Nam, C.W.; Chung, I.S. Spatial analysis between particulate matter and emergency room visits for conjunctivitis and keratitis. *Ann. Occup. Environ. Med.* **2018**, *30*, 41. [CrossRef]
18. Sendra, V.G.; Tau, J.; Zapata, G.; Vitar, R.M.L.; Illian, E.; Chiaradía, P.; Berra, A. Polluted Air Exposure Compromises Corneal Immunity and Exacerbates Inflammation in Acute Herpes Simplex Keratitis. *Front. Immunol.* **2021**, *12*, 618597. [CrossRef]
19. Manisalidis, I.; Stavropoulou, E.; Stavropoulos, A.; Bezirtzoglou, E. Environmental and Health Impacts of Air Pollution: A Review. *Front. Public Health* **2020**, *20*, 14. [CrossRef]
20. Mo, Z.; Fu, Q.; Lyu, D.; Zhang, L.; Qin, Z.; Tang, Q.; Yin, H.; Xu, P.; Wu, L.; Wang, X.; et al. Impacts of air pollution on dry eye disease among residents in Hangzhou, China: A case-crossover study. *Environ. Pollut.* **2019**, *246*, 183–189. [CrossRef]
21. Klopfer, J. Effects of environmental air pollution on the eye. *J. Am. Optom. Assoc.* **1989**, *60*, 773–778.
22. Torricelli, A.A.; Matsuda, M.; Novaes, P.; Braga, A.L.; Saldiva, P.H.; Alves, M.R.; Monteiro, M.L. Effects of ambient levels of traffic-derived air pollution on the ocular surface: Analysis of symptoms, conjunctival goblet cell count and mucin 5AC gene expression. *Environ. Res.* **2014**, *131*, 59–63. [CrossRef]
23. Chang, C.J.; Yang, H.H.; Chang, C.A.; Tsai, H.Y. Relationship between air pollution and outpatient visits for nonspecific conjunctivitis. *Invest. Ophthalmol. Vis. Sci.* **2012**, *53*, 429–433. [CrossRef]
24. Chang, C.J.; Yang, H.H. Impact on Eye Health Regarding Gaseous and Particulate Pollutants. *Aerosol Air Qual. Res.* **2020**, *20*, 1695–1699.
25. Li, L.; Xing, C.; Zhou, J.; Niu, L.; Luo, B.; Song, M.; Niu, J.; Ruan, Y.; Sun, X.; Lei, Y. Airborne particulate matter (PM2.5) triggers ocular hypertension and glaucoma through pyroptosis. *Part. Fibre Toxicol.* **2021**, *18*, 10. [CrossRef]
26. Chirino, Y.I.; Sánchez-Pérez, Y.; Osornio-Vargas, A.R.; Morales-Bárcenas, R.; Gutiérrez-Ruíz, M.C.; Segura-García, Y.; Rosas, I.; Pedraza-Chaverri, J.; García-Cuellar, C.M. PM(10) impairs the antioxidant defense system and exacerbates oxidative stress driven cell death. *Toxicol. Lett.* **2010**, *193*, 209–216. [CrossRef]
27. Ha, J.W.; Boo, Y.C. Siegesbeckiae Herba Extract and Chlorogenic Acid Ameliorate the Death of HaCaT Keratinocytes Exposed to Airborne Particulate Matter by Mitigating Oxidative Stress. *Antioxidants* **2021**, *10*, 1762. [CrossRef]
28. Bortey-Sam, N.; Ikenaka, Y.; Akoto, O.; Nakayama, S.M.M.; Asante, K.A.; Baidoo, E.; Obirikorang, C.; Saengtienchai, A.; Isoda, N.; Nimako, C.; et al. Oxidative stress and respiratory symptoms due to human exposure to polycyclic aromatic hydrocarbons (PAHs) in Kumasi, Ghana. *Environ. Pollut.* **2017**, *228*, 311–320. [CrossRef]
29. Vinzents, P.S.; Møller, P.; Sørensen, M.; Knudsen, L.E.; Hertel, O.; Jensen, F.P.; Schibye, B.; Loft, S. Personal exposure to ultrafine particles and oxidative DNA damage. *Environ. Health Perspect.* **2005**, *113*, 1485–1490. [CrossRef]
30. Donaldson, K.; Brown, D.M.; Mitchell, C.; Dineva, M.; Beswick, P.H.; Gilmour, P.; MacNee, W. Free radical activity of PM10: Iron-mediated generation of hydroxyl radicals. *Environ. Health Perspect.* **1997**, *105* (Suppl. 5), 1285–1289. [CrossRef]

31. Zheng, L.; Liu, S.; Zhuang, G.; Xu, J.; Liu, Q.; Zhang, X.; Deng, C.; Guo, Z.; Zhao, W.; Liu, T.; et al. Signal Transductions of BEAS-2B Cells in Response to Carcinogenic PM2.5 Exposure Based on a Microfluidic System. *Anal. Chem.* **2017**, *89*, 5413–5421. [CrossRef]
32. Pardo, M.; Qiu, X.; Zimmermann, R.; Rudich, Y. Particulate Matter Toxicity Is Nrf2 and Mitochondria Dependent: The Roles of Metals and Polycyclic Aromatic Hydrocarbons. *Chem. Res. Toxicol.* **2020**, *33*, 1110–1120. [CrossRef]
33. Harmon, A.C.; Hebert, V.Y.; Cormier, S.A.; Subramanian, B.; Reed, J.R.; Backes, W.L.; Dugas, T.R. Particulate matter containing environmentally persistent free radicals induces AhR-dependent cytokine and reactive oxygen species production in human bronchial epithelial cells. *PLoS ONE* **2018**, *13*, e0205412. [CrossRef]
34. Skulachev, V.P. Cationic antioxidants as a powerful tool against mitochondrial oxidative stress. *Biochem. Biophys. Res. Commun.* **2013**, *441*, 275–279. [CrossRef]
35. Ježek, J.; Engstová, H.; Ježek, P. Antioxidant mechanism of mitochondria-targeted plastoquinone SkQ1 is suppressed in aglycemic HepG2 cells dependent on oxidative phosphorylation. *Biochim. Biophys. Acta Bioenerg.* **2017**, *1858*, 750–762. [CrossRef]
36. Severin, F.F.; Severina, I.I.; Antonenko, Y.N.; Rokitskaya, T.I.; Cherepanov, D.A.; Mokhova, E.N.; Vyssokikh, M.Y.; Pustovidko, A.V.; Markova, O.V.; Yaguzhinsky, L.S.; et al. Penetrating cation/fatty acid anion pair as a mitochondria-targeted protonophore. *Proc. Natl. Acad. Sci. USA* **2010**, *107*, 663–668. [CrossRef]
37. Kezic, A.; Spasojevic, I.; Lezaic, V.; Bajcetic, M. Mitochondria-Targeted Antioxidants: Future Perspectives in Kidney Ischemia Reperfusion Injury. *Oxid. Med. Cell Longev.* **2016**, *2016*, 2950503. [CrossRef]
38. Skulachev, V.P. SkQ1 treatment and food restriction–two ways to retard an aging program of organisms. *Aging* **2011**, *3*, 1045–1050. [CrossRef]
39. Genrikhs, E.E.; Stelmashook, E.V.; Popova, O.V.; Kapay, N.A.; Korshunova, G.A.; Sumbatyan, N.V.; Skrebitsky, V.G.; Skulachev, V.P.; Isaev, N.K. Mitochondria-targeted antioxidant SkQT1 decreases trauma-induced neurological deficit in rat and prevents amyloid-β-induced impairment of long-term potentiation in rat hippocampal slices. *J. Drug Target.* **2015**, *23*, 347–352. [CrossRef]
40. Zernii, E.Y.; Gancharova, O.S.; Baksheeva, V.E.; Golovastova, M.O.; Kabanova, E.I.; Savchenko, M.S.; Tiulina, V.V.; Sotnikova, L.F.; Zamyatnin, A.A., Jr.; Philippov, P.P.; et al. Mitochondria-Targeted Antioxidant SkQ1 Prevents Anesthesia-Induced Dry Eye Syndrome. *Oxid. Med. Cell. Longev.* **2017**, *2017*, 9281519. [CrossRef]
41. Brzheskiy, V.V.; Efimova, E.L.; Vorontsova, T.N.; Alekseev, V.N.; Gusarevich, O.G.; Shaidurova, K.N.; Ryabtseva, A.A.; Andryukhina, O.M.; Kamenskikh, T.G.; Sumarokova, E.S.; et al. Results of a Multicenter, Randomized, Double-Masked, Placebo-Controlled Clinical Study of the Efficacy and Safety of Visomitin Eye Drops in Patients with Dry Eye Syndrome. *Adv. Ther.* **2015**, *32*, 1263–1279. [CrossRef]
42. Song, S.J.; Hyun, S.W.; Lee, T.G.; Park, B.; Jo, K.; Kim, C.S. New application for assessment of dry eye syndrome induced by particulate matter exposure. *Ecotoxicol. Environ. Saf.* **2020**, *205*, 111125. [CrossRef]
43. Yu, D.; Deng, Q.; Wang, J.; Chang, X.; Wang, S.; Yang, R.; Yu, J.; Yu, J. Air Pollutants are associated with Dry Eye Disease in Urban Ophthalmic Outpatients: A Prevalence Study in China. *J. Transl. Med.* **2019**, *17*, 46. [CrossRef]
44. Tan, G.; Li, J.; Yang, Q.; Wu, A.; Qu, D.Y.; Wang, Y.; Ye, L.; Bao, J.; Shao, Y. Air pollutant particulate matter 2.5 induces dry eye syndrome in mice. *Sci. Rep.* **2018**, *8*, 17828.
45. Kang, W.S.; Choi, H.; Jang, G.; Lee, K.H.; Kim, E.; Kim, K.J.; Jeong, G.-Y.; Kim, J.S.; Na, C.-S.; Kim, S. Long-Term Exposure to Urban Particulate Matter on the Ocular Surface and the Incidence of Deleterious Changes in the Cornea, Conjunctiva and Retina in Rats. *Int. J. Mol. Sci.* **2020**, *21*, 4976. [CrossRef]
46. Schantz, M.M.; Cleveland, D.; Heckert, N.A.; Kucklick, J.R.; Leigh, S.D.; Long, S.E.; Lynch, J.M.; Murphy, K.E.; Olfaz, R.; Pintar, A.L.; et al. Development of two fine particulate matter standard reference materials (<4 μm and <10 μm) for the determination of organic and inorganic constituents. *Anal. Bioanal. Chem.* **2016**, *408*, 4257–4266. [CrossRef]
47. Li, J.; Tan, G.; Ding, X.; Wang, Y.; Wu, A.; Yang, Q.; Ye, L.; Shao, Y. A mouse dry eye model induced by topical administration of the air pollutant particulate matter 10. *Biomed. Pharmacother.* **2017**, *96*, 524–534. [CrossRef]
48. Mu, N.; Wang, H.; Chen, D.; Wang, F.; Ji, L.; Zhang, C.; Li, M.; Lu, P. A Novel Rat Model of Dry Eye Induced by Aerosol Exposure of Particulate Matter. *Invest. Ophthalmol. Vis. Sci.* **2022**, *63*, 39. [CrossRef]
49. Bourcier, T.; Acosta, M.C.; Borderie, V.; Borrás, F.; Gallar, J.; Bury, T.; Laroche, L.; Belmonte, C. Decreased corneal sensitivity in patients with dry eye. *Invest. Ophthalmol. Vis. Sci.* **2005**, *46*, 2341–2345. [CrossRef]
50. Radan, M.; Dianat, M.; Badavi, M.; Mard, S.A.; Bayati, V.; Goudarzi, G. In vivo and in vitro evidence for the involvement of Nrf2-antioxidant response element signaling pathway in the inflammation and oxidative stress induced by particulate matter (PM10): The effective role of gallic acid. *Free. Radic. Res.* **2019**, *53*, 210–225. [CrossRef]
51. Wu, S.; Lu, H.; Bai, Y. Nrf2 in cancers: A double-edged sword. *Cancer Med.* **2019**, *8*, 2252–2267. [CrossRef]
52. Singh, A.; Rangasamy, T.; Thimmulappa, R.K.; Lee, H.; Osburn, W.O.; Brigelius-Flohé, R.; Kensler, T.W.; Yamamoto, M.; Biswal, S. Glutathione peroxidase 2, the major cigarette smoke-inducible isoform of GPX in lungs, is regulated by Nrf2. *Am. J. Respir. Cell. Mol. Biol.* **2006**, *35*, 639–650. [CrossRef]
53. Shih, A.Y.; Johnson, D.A.; Wong, G.; Kraft, A.D.; Jiang, L.; Erb, H.; Johnson, J.A.; Murphy, T.H. Coordinate regulation of glutathione biosynthesis and release by Nrf2-expressing glia potently protects neurons from oxidative stress. *J. Neurosci.* **2003**, *23*, 3394–3406. [CrossRef]

54. Pantoja, I.E.M.; Hu, C.-L.; Perrone-Bizzozero, N.I.; Zheng, J.; Bizzozero, O.A. Nrf2-dysregulation correlates with reduced synthesis and low glutathione levels in experimental autoimmune encephalomyelitis. *J. Neurochem.* **2016**, *139*, 640–650. [CrossRef]
55. Lee, H.; Kim, D.H.; Hwangbo, H.; Kim, S.Y.; Ji, S.Y.; Kim, M.Y.; Shim, J.-H.; Leem, S.-H.; Hyun, J.W.; Kim, G.-Y.; et al. The Protective Effect of Topical Spermidine on Dry Eye Disease with Retinal Damage Induced by Diesel Particulate Matter2.5. *Pharmaceutics* **2021**, *13*, 1439. [CrossRef]
56. Lee, T.G.; Hyun, S.W.; Jo, K.; Park, B.; Lee, I.S.; Song, S.J.; Kim, C.S. Achyranthis radix Extract Improves Urban Particulate Matter-Induced Dry Eye Disease. *Int. J. Environ. Res. Public Health* **2019**, *16*, 3229. [CrossRef]
57. Vnukov, V.V.; Gutsenko, O.I.; Milyutina, N.P.; Kornienko, I.V.; Ananyan, A.A.; Plotnikov, A.A.; Panina, S.B. SkQ1 Regulates Expression of Nrf2, ARE-Controlled Genes Encoding Antioxidant Enzymes, and Their Activity in Cerebral Cortex under Oxidative Stress. *Biochemistry* **2017**, *82*, 942–952. [CrossRef]
58. Yoon, S.; Han, S.; Jeon, K.J.; Kwon, S. Effects of collected road dusts on cell viability, inflammatory response, and oxidative stress in cultured human corneal epithelial cells. *Toxicol. Lett.* **2018**, *284*, 152–160. [CrossRef]
59. Wei, Y.; Troger, A.; Spahiu, V.; Perekhvatova, N.; Skulachev, M.; Petrov, A.; Chernyak, B.; Asbell, P. The Role of SKQ1 (Visomitin) in Inflammation and Wound Healing of the Ocular Surface. *Ophthalmol. Ther.* **2019**, *8*, 63–73. [CrossRef]
60. Lodovici, M.; Bigagli, E. Oxidative stress and air pollution exposure. *J. Toxicol.* **2011**, *2011*, 487074. [CrossRef]
61. Visalli, G.; Baluce, B.; Bertuccio, M.; Picerno, I.; Di Pietro, A. Mitochondrial-mediated apoptosis pathway in alveolar epithelial cells exposed to the metals in combustion-generated particulate matter. *J. Toxicol. Environ. Health A* **2015**, *78*, 697–709. [CrossRef]
62. Gualtieri, M.; Mantecca, P.; Corvaja, V.; Longhin, E.; Perrone, M.G.; Bolzacchini, E.; Camatini, M. Winter fine particulate matter from Milan induces morphological and functional alterations in human pulmonary epithelial cells (A549). *Toxicol. Lett.* **2009**, *188*, 52–62. [CrossRef]
63. Leclercq, B.; Kluza, J.; Antherieu, S.; Sotty, J.; Alleman, L.Y.; Perdrix, E.; Loyens, A.; Coddeville, P.; Lo Guidice, J.M.; Marchetti, P.; et al. Air pollution-derived PM2.5 impairs mitochondrial function in healthy and chronic obstructive pulmonary diseased human bronchial epithelial cells. *Environ. Pollut.* **2018**, *243 Pt B*, 1434–1449. [CrossRef]
64. Cattani-Cavalieri, I.; Valenca, S.S.; Lanzetti, M.; Carvalho, G.M.C.; Zin, W.A.; Monte-Alto-Costa, A.; Porto, L.C.; Romana-Souza, B. Acute Exposure to Diesel-Biodiesel Particulate Matter Promotes Murine Lung Oxidative Stress by Nrf2/HO-1 and Inflammation Through the NF-kB/TNF-α Pathways. *Inflammation* **2019**, *42*, 526–537. [CrossRef]
65. Wang, Y.; Zhang, M.; Li, Z.; Yue, J.; Xu, M.; Zhang, Y.; Yung, K.K.L.; Li, R. Fine particulate matter induces mitochondrial dysfunction and oxidative stress in human SH-SY5Y cells. *Chemosphere* **2019**, *218*, 577–588. [CrossRef]
66. Torricelli, A.A.; Novaes, P.; Matsuda, M.; Alves, M.R.; Monteiro, M.L. Ocular surface adverse effects of ambient levels of air pollution. *Arq. Bras. Oftalmol.* **2011**, *74*, 377–381. [CrossRef]
67. Cao, S.R.; Chen, Y.Y.; Ren, G.Y.; Li, S.M. Analysis of organic and inorganic components of inhalable particles in the atmosphere. *Biomed. Environ. Sci.* **1988**, *1*, 130–137.
68. Ko, H.M.; Choi, S.H.; Kim, Y.; An, E.J.; Lee, S.H.; Kim, K.; Jung, H.J.; Jang, H.J. Effect of Rosa laevigata on PM10-Induced Inflammatory Response of Human Lung Epithelial Cells. *Evid.-Based Complement. Altern. Med.* **2020**, *2020*, 2893609. [CrossRef]
69. Ha, J.W.; Song, H.; Hong, S.S.; Boo, Y.C. Marine Alga Ecklonia cava Extract and Dieckol Attenuate Prostaglandin E2 Production in HaCaT Keratinocytes Exposed to Airborne Particulate Matter. *Antioxidants* **2019**, *8*, 190. [CrossRef]
70. De Silva, M.E.H.; Hill, L.J.; Downie, L.E.; Chinnery, H.R. The Effects of Aging on Corneal and Ocular Surface Homeostasis in Mice. *Invest. Ophthalmol. Vis. Sci.* **2019**, *60*, 2705–2715. [CrossRef]
71. Kimura, Y.; Kimura, H. Hydrogen sulfide protects neurons from oxidative stress. *FASEB J.* **2004**, *18*, 1165–1167. [CrossRef]
72. Huang, X.; Barrett, R.P.; McClellan, S.A.; Hazlett, L.D. Silencing Toll-like receptor-9 in Pseudomonas aeruginosa keratitis. *Invest. Ophthalmol. Vis. Sci.* **2005**, *46*, 4209–4216. [CrossRef]
73. Somayajulu, M.; Ekanayaka, S.; McClellan, S.A.; Bessert, D.; Pitchaikannu, A.; Zhang, K.; Hazlett, L.D. Airborne Particulates Affect Corneal Homeostasis and Immunity. *Invest. Ophthalmol. Vis. Sci.* **2020**, *61*, 23. [CrossRef] [PubMed]
74. Kido, K.; Ito, H.; Yamamoto, Y.; Makita, K.; Uchida, T. Cytotoxicity of propofol in human induced pluripotent stem cell-derived cardiomyocytes. *J. Anesth.* **2018**, *32*, 120–131. [CrossRef] [PubMed]